AD-A042 698 VIRGINIA UNIV CHARLOTTESVILLE SCHOOL OF ENGINEERING--ETC F/G 20/3
STABILITY DERIVATIVE MEASUREMENTS FOR MAGNETICALLY SUSPENDED CO--ETC(U)
JAN 77 D BHARATHAN, S S FISHER AF-AFOSR-2705-74

UNCLASSIFIED AFOSR-TR-77-0666 NL

| OF |
AD
A042698

END
DATE FILMED
8-77
DDC

77-79

Stability Derivative Measurements for Magnetically Suspended Cone-Cylinder Models

D. Bharathan, *Dartmouth College, Hanover, N.H.; and* S.S. Fisher, *University of Virginia, Charlottesville, Va.*

AIAA 15th AEROSPACE SCIENCES MEETING

Los Angeles, Calif./January 24-26, 1977

See 1473

STABILITY DERIVATIVE MEASUREMENTS WITH MAGNETICALLY SUSPENDED CONE-CYLINDER MODELS*

D.Bharathan** and S.S.Fisher+
University of Virginia, Charlottesville, VA 22901

ABSTRACT

In an initial feasibility study, the stability derivatives, C_{m_α}, $C_{m_{\dot{\alpha}}} + C_{m_q}$, C_{z_α} and $C_{z_{\dot{\alpha}}} + C_{z_q}$ for 5- and 7-caliber cone-cylinder models have been measured at M = 0.071 and Re = 1.3×10^4 by suspending each model electromagnetically in a small subsonic wind tunnel, forcing it in periodic, combined pitching/heaving motion at frequencies near pitch resonance, and comparing its frequency response with flow to that without flow. Drag coefficients are measured as well. The apparatus and techniques employed are described, the analytical model used to extract the derivatives from the response data is outlined, typical response data are shown, comparisons are made with conventionally obtained, similar data from other facilities, and a general assessment of the technique is made.

INTRODUCTION

Preliminary stability evaluations for aerodynamic vehicles are usually carried out either with sting-mounted models in wind tunnels or with models in free flight. In wind-tunnel tests, the influence of the sting can be significant and in free-flight tests observation time usually is severely limited and data retrieval is difficult. On the otherhand, magnetic suspension of wind-tunnel models eliminates the fluid-mechanics aspects of sting interference without incurring the complexities of free-flight testing.

The present investigation represents an initial application to stability testing of an electromagnetic suspension system which has been operated at the University of Virginia over the past ten years. It follows only a very few stability investigations of somewhat limited scope conducted with magnetically suspended models elsewhere, (1-4). These tests are aimed primarily at evaluating the practicality of measuring stability derivatives with this apparatus. For the experiments, the nominal objective was to measure the pitching-moment derivative and, particularly, the pitch-damping derivative for each model. After an analytical model for the motion was developed and the data were obtained, it was found that side-force and side-moment-damping derivatives also could be estimated.

APPARATUS

The electromagnetic coil arrangement for the suspension system is shown in Figure 1. A large pair of Helmholtz coils produces a uniform field to magnetize the model and a second pair of opposed coils creates a streamwise (vertical) gradient in the field at the configuration centroid, the nominal model-support location. This gradient induces a force on the model which opposes its weight and drag. Third and fourth sets of coils create lateral (horizontal) gradients in the field which induce side forces on the model. The Helmholtz coils carry up to 200 A and produce a field of up to 120,000 A/m at the model location. The vertical gradient coils carry up to 150 A and produce a field gradient as high as 390,000 A/m² at the model. The horizontal gradient coils carry up to 45 A and produce a gradient as high as 9,500 A/m² at the model. All coils are water cooled.

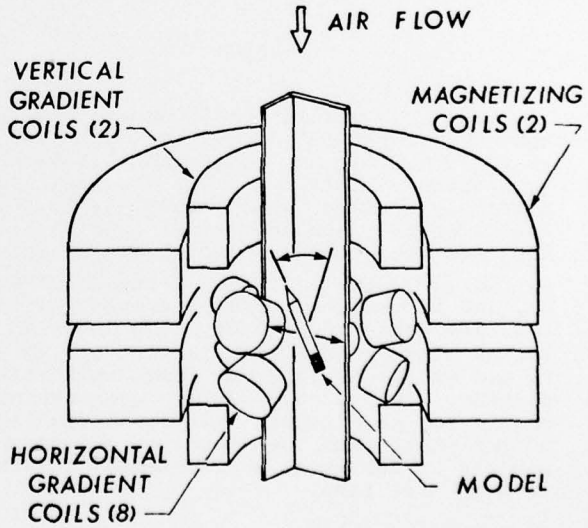

Figure 1 Electromagnetic Suspension Apparatus

*Research supported by AFOSR Grant 74-2705.

**Research Assistant. Now Research Associate, Thayer School of Engineering, Dartmouth College, Hanover, N.H., Student Member, AIAA.

+Associate Professor, Engineering Science and Systems. Now Visiting Staff Member, Applied Photochemistry Division, Los Alamos Scientific Laboratory.

The wind-tunnel test section is inserted inside the group of coils. This tunnel is a small, fan-driven, open-return tunnel with high contraction ratio. The test section is 11.4 cm by 11.4 cm by 30.0 cm long, the air speed for these tests was 24 m/s, and the flow turbulence level was 0.4%.

Model position is sensed optically using parallel light beams and silicon photocells. A feedback control system is then used to keep the model centered near its nominal support location. For this, feedback signals indicative of the model's position along each of three orthogonal axes, after passing through appropriate compensating electronic networks, drive power amplifiers supplying current to respective sets of force coils.

For the stability tests, the model is forced periodically in combined pitching and heaving motion. Here, model pitch orientation is monitored by sensing its lateral position at separate stations along its length. To reduce the effects of noise (due primarily to flow turbulence and secondarily to structural vibration and control-system noise), a 256-channel digital signal averager was used and the several position-sensor and coil-current waveforms were averaged simultaneously by multiplexing the input to the averager.

Other details concerning the apparatus as well as a more complete review of its operation and development are given in Ref. 5.

MODELS

The two models employed are simple cone-cylinders. For each, the nose is a sharp cone 15.2 mm long with 14.5 degree semivertex angle. The cylindrical afterbody, 7.8 mm in diameter, is 22.9 mm long for the 5-caliber model and 38.3 mm long for the 7-caliber model. The cylinder is hollow, with an inner diameter of 6.9 mm, and is machined from a single Lucite rod. The magnetic part of each model is a hollow steel (AISI-01) cylinder 6.9 mm OD by 6.3 mm ID by 12.7 mm long which fits tightly inside the outer aerodynamic shell. For each model, the downstream end of the shell and the core are coincident and the model base is carefully covered with plastic tape.

The models are made axisymmetric because model roll is uncontrolled in this suspension system, and position control and sensing would be prohibitively difficult for a rolling, non-symmetric model. The overall size of the model and core are limited by the wind tunnel's size (which is in turn limited by the space available between the coils) and the size of the region over which the magnetic field gradients are approximately constant. The relative sizing and mass of the aerodynamic shell and magnetic core, together with the imposed magnetic field, are chosen to place the model's pitch-resonance frequency above the bandwidth of the position-control system, allow for a reasonably large aerodynamic drag, and keep the electromagnetic damping small. This selection leaves the control system's effectiveness essentially unaltered, while permitting adequate forced-motion amplitudes to be achieved rather readily near pitch resonance.

PROCEDURE

For the tests, the model is driven magnetically with a sinusoidal lateral force over a series of frequencies covering pitch resonance. Due to the fact that the centers of mass of the model shell and core are not coincident, the excitation force induces a combined pitching and heaving motion (predominantly pitching, since this motion is lightly damped). To simplify interpretation of the overall motion, the pitch-angle amplitude is always kept small, less than 0.5 degree. Thus non-linear aerodynamic and electromagnetic effects on the model motion are minimized. This also allows a number of cross-coupled electromagnetic forces and moments acting on the model to be neglected. A theoretical model for the model's response is then used to extract estimates for unknown aerodynamic and electromagnetic coefficients. This model provides analytical expressions for the model's transfer functions in pitch and in heave. These expressions are algebraic functions of the aerodynamic and electromagnetic coefficients and the unknown coefficients are determined by fitting the measured data to these expressions in a least square sense.

Transfer-function amplitudes and phases are obtained upon computer processing the recorded averaged position-sensor waveforms and coil-current waveforms. In this, measured position-sensor and force-current calibrations are used to convert raw-signal data to positions, angles, velocities, and forces.

Data processing yields plots versus frequency of (1) transfer-function amplitudes, θ_0/F_0 and w_0/F_0 where θ_0 is the pitch amplitude, w_0 is the non-dimensional heave velocity amplitude, and F_0 is the non-dimensional perturbing force amplitude, and (2) transfer-function phase angles ϕ_θ and ϕ_w, the angles by which the pitch orientation and the heave velocity lead the perturbing force. *

Transfer function variations are measured both with flow and without flow. Simple flow-off (rather than vacuum) measurements are satisfactory here because still-air damping is negligible compared to electromagnetic damping. From the flow-off data, the unknown electromagnetic force and moment coefficients are determined and, once these are known, the aerodynamic force and moment coefficients can be determined from the flow-on data.

THEORETICAL TRANSFER FUNCTIONS

In Ref. 5, the following analytical expressions for the model transfer functions are derived:

$$\frac{w}{F} = \frac{P_1[\, s^2 + 2P_2P_3 s + P_3^2 \,]}{s\,[\, s^2 + 2P_5P_6 s + P_6^2 \,]} \qquad (1)$$

$$\frac{\theta}{F} = \frac{P_4}{[\, s^2 + 2P_5P_6 s + P_6^2 \,]} \qquad (2)$$

where

$$P_1 = 1/2\mu$$

$$P_3^2 = [\, k + 2\mu g a - C_{m_\alpha} - aC_{z_\alpha} \,]/i_B$$

$$2P_2P_3 = [\varepsilon_m - a(C_{z_{\dot\alpha}} + C_{z_q}) - (C_{m_{\dot\alpha}} + C_{m_q})]/i_B$$

$$P_4 = -a/i_B$$

$$P_6^2 = [k + \gamma_x I_{x_0}(1+n)a - C_{m_\alpha}]/i_B$$

$$2P_5P_6 = [\varepsilon_m + a^2\varepsilon_z - (C_{m_{\dot\alpha}} + C_{m_q})]/i_B$$

In these expressions, P_3 and P_6 represent natural frequencies, P_2 and P_5 represent the associated damping factors, and P_1 and P_4 are proportionality constants.

---

* In this work, velocity is normalized with the airspeed, V, and electromagnetic lateral force is normalized with the flow dynamic pressure times the model base area. For the aerodynamic parameters, the model base diameter is used as the normalizing length.

Here,

- a = axial distance between the model's center of mass and center of magnetization,
- $C_{m_\alpha}, C_{m_{\dot\alpha}}, C_{m_q}$ = aerodynamic pitching moment derivatives,
- $C_{z_\alpha}, C_{z_{\dot\alpha}}, C_{z_q}$ = aerodynamic side-force derivatives,
- g = gravitational acceleration,
- I_{x_0} = vertical gradient-coil current,
- i_B = model moment of inertia,
- k = magnetic pitch stiffness,
- n = core shape factor, $(1-3N_x)/2(1-N_x)$
- N_x = core axial demagnetizing factor,
- s = Laplace transform variable,
- γ_x = vertical coil force constant,
- ε_m = magnetic damping moment coefficient,
- ε_z = magnetic damping force coefficient,
- μ = model mass.

In developing these expressions, as justified in Ref. 5, the effect of the heaving motion on the pitching motion is neglected. i.e. the pitching motion is treated as that for a simple linear damped oscillator. Also, magnetic damping in pitch and heave are assumed linearly proportional to the pitching angular velocity and the heaving velocity, respectively. For the small motion amplitudes here, these latter assumption are satisfactorily accurate.

TRANSFER FUNCTION DATA

Measured flow-off variations for the pitch transfer function for the 5-caliber model are shown in Figure 2. The data in this figure and following figures are taken from four sets of independent runs, two each for excitation along a separate lateral axis. Since within the scatter in the data the four sets identical, all data have been combined. For presentation, the phase data is plotted as $\cos\phi$ rather than ϕ itself. The plotted curve through the amplitude data is a least-squares fitted version of Eq.(2). A standard computer code (6) was used to obtain this fit. Using the values of P_i (i=1,6) determined for this match, the curve through the phase data is obtained, i.e. the phase curve is not a least-squares fit to the phase data , but is that corresponding to the P_i values determined from the amplitude match. Of course, the plotted curves in this figure are merely those for resonance of a simple damped oscillator. The amplitude exhibits a sharp peak at the resonant frequency and across this peak the phase changes rapidly by 180 degrees. The excellent agreement between the plotted curves and the data is convincing evidence that the pitching motion is properly modeled.

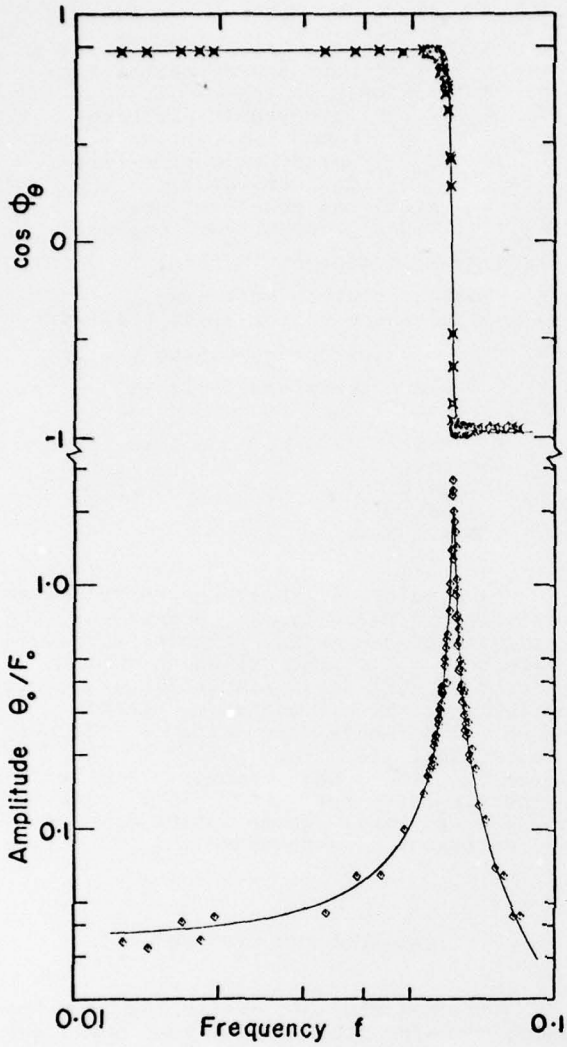

Figure 2 Pitch Transfer Function
5-Caliber Model, Flow Off

Flow-off heave transfer function data for this model are shown in Figure 3. The curve plotted through the amplitude data in this figure is the least-squares fitted variation of Eq.(1) and the curve accompanying the phase data is that corresponding to the P_i values determined from the amplitude match. The sharp excursions in the amplitude data show that, while the effect of heave on pitch near resonance can be neglected, the reverse effect cannot. This excursion occurs because the net side force on the model is the sum of the imposed force, F, and a second component, with both magnetic and gravitational contributions, induced by model pitch. Below resonance, θ and F are in phase, the two components add, and the heave amplitude increases with increasing pitch amplitude. Above resonance, θ and F are 180 degrees out of phase and the result is the observed dip.

At frequencies well below resonance, as would be expected, cos ϕ_w approaches zero, corresponding to ϕ_w=-90 degrees. The dip in cos ϕ_w just below resonance is due to pitch-heave coupling. The measured overshoot in cos ϕ_w just above resonance is probably not real. It could easily be a result of inaccuracies in the phase measurement which become large wherever w_0 is small . The slight drop in the cos ϕ_w data below the predicted curve with increasing f also may not be real. Except near resonance, w decreases roughly as the inverse of f, thus leading to increased inaccuracies in ϕ_w measurements. Since P_i values are determined from matches to the more accurate amplitude data, these possible phase-measurement errors are relatively unimportant.

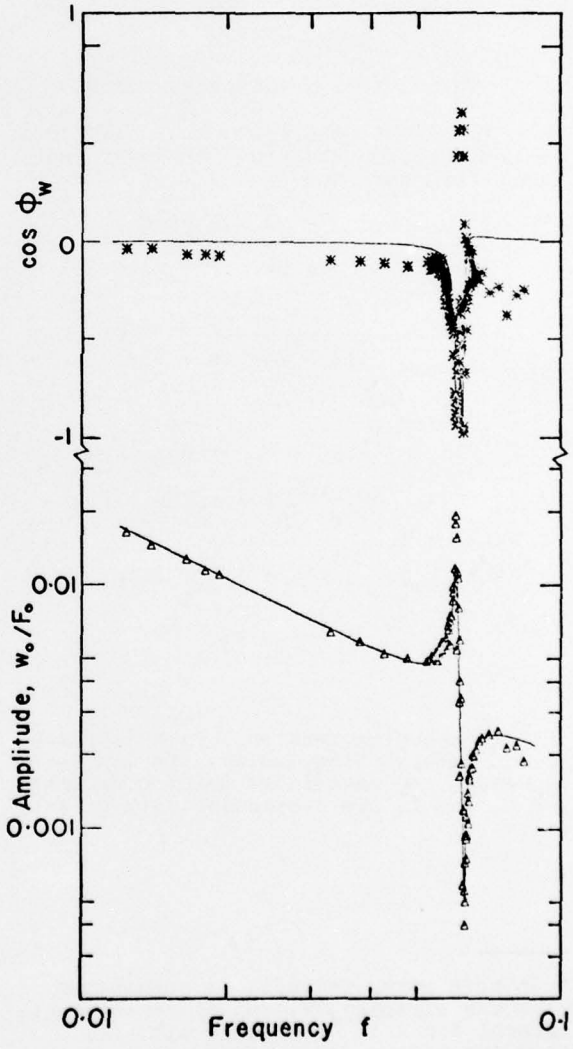

Figure 3 Heave Transfer Function
5-Caliber Model, Flow Off

Corresponding flow-on response data for this model are shown in Figures 4 and 5. Again, the lines through the amplitude data are fitted and the lines through the phase data are predicted on the basis of the amplitude matches. These flow-on data are quite similar to the flow-off data. With the flow on, the pitch resonance frequency is reduced slightly due to the presence of the destabilizing aerodynamic pitching moment, and the width of the resonance peak is slightly increased due to aerodynamic damping. Also, the excursion in the heave amplitude near pitch resonance is inverted. This inversion indicates that the aerodynamic side force (primarily due to C_{z_α}) is opposite in sign to and greater in magnitude than the sum of the magnetic and gravitational side forces. The noted disagreement between measured and predicted values of cos ϕ_w is again attributed to high ϕ_w measurement error where w_0 is small.

Similar transfer function data and fits have also been obtained for the 7-caliber model and they are presented in Ref. 5.

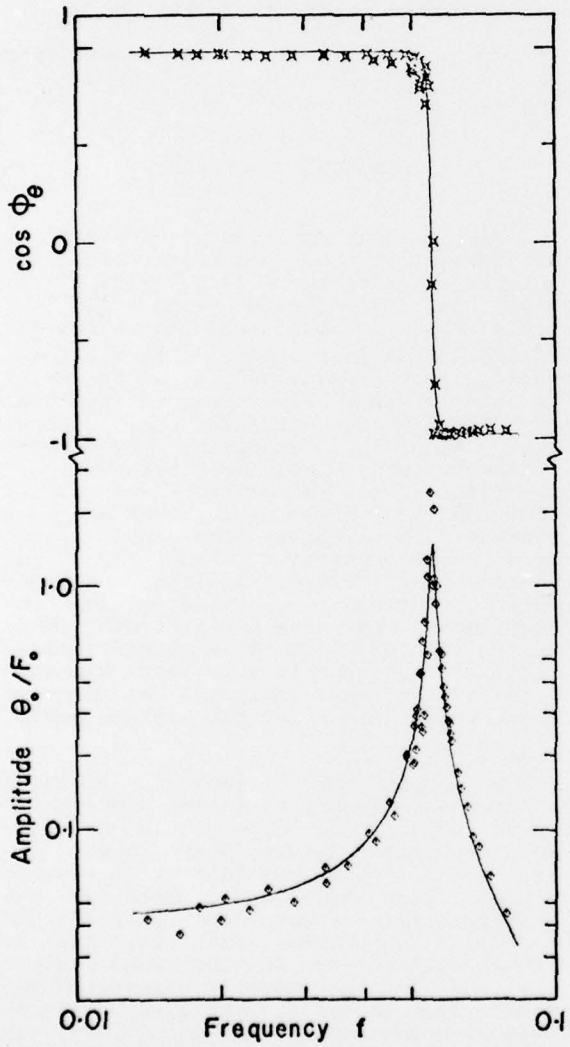

Figure 4 Pitch Transfer Function
5-Caliber Model, Flow On

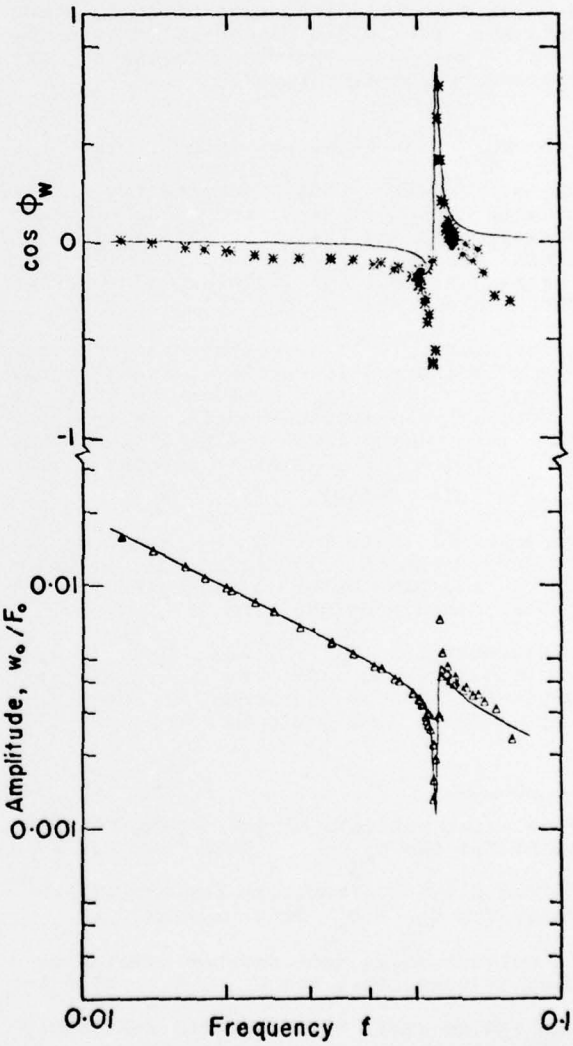

Figure 5 Heave Transfer Function
5-Caliber Model, Flow On

STABILITY DERIVATIVES

Deduced values of C_{z_α}, C_{m_α}, $C_{z_{\dot{\alpha}}} + C_{z_q}$ and $C_{m_{\dot{\alpha}}} + C_{m_q}$ are listed in Tables 1 and 2. Values of the axial force (negative drag) coefficient, C_x, also measured in these experiments, are listed as well. Analytical estimates and comparable measurements obtained elsewhere are also included. The analytical estimates are taken from the USAF DATCOM (Data Compendium) (7) and, except for C_x are based on an assumption of inviscid flow over a slender body. No comparable data for $C_{z_{\dot{\alpha}}} + C_{z_q}$ for either model could be found in the literature, and comparable $C_{m_{\dot{\alpha}}} + C_{m_q}$ data could be found only for the 5-caliber model. Also, none of these other data are for exact matches of M, Re, or model shape. These parameters are reasonably close, however.

For the 5-caliber model, the C_{z_α} value, with 60% uncertainty (1σ uncertainty), is 75% of the mean of other measurements and 20% below its analytical estimate; the large uncertainty for this measurement could readily explain either difference. The C_{m_α} value, with 3% uncertainty, is 3% above the mean of other measurements and 10% above its analytical estimate. The C_x value, with 2% uncertainty, compares well with its laminar analytical estimate, thus indicating a fully laminar boundary layer over this model. The $C_{m_{\dot{\alpha}}} + C_{m_q}$ measurement, with 50% uncertainty, is 10% below its analytical estimate and at least is of the same order of magnitude as the other measurements*. The $C_{z_{\dot{\alpha}}} + C_{z_q}$ measurement, with essentially 100% uncertainty, is 30% of its analytical estimate, and, as mentioned, no comparable experimental data could be found.

For the 7-caliber model, the measured C_{z_α} value, with 10% uncertainty, is 30% higher than its analytical estimate and 10% above the mean of the other measurements. The C_{m_α} value, with 3% uncertainty, is 15% below its analytical estimate and 10% below the mean of the other measurements. The C_x measurement, with 2% uncertainty, lies between the two analytical estimates, one assuming fully turbulent and the other fully laminar flow. This suggests a partially turbulent boundary layer over this longer model. The $C_{m_{\dot{\alpha}}} + C_{m_q}$ measurement, with 25% uncertainty, is 25% greater than its analytical estimate. The $C_{z_{\dot{\alpha}}} + C_{z_q}$ value, with essentially 100% uncertainty, is 30% of its analytical estimate. As already mentioned, no comparable data for $C_{m_{\dot{\alpha}}} + C_{m_q}$ or $C_{z_{\dot{\alpha}}} + C_{z_q}$ for this model were found.

CONCLUDING REMARKS

The present experiments demonstrate the feasibility of measuring selected stability derivatives in this facility. They also illustrate some of the complexities involved and some typical measurement uncertainty levels. For these models, they provide additional estimates for some of the aerodynamic derivatives and entirely new estimates for others. Since the main objective of these experiments was to measure pitching-moment and pitch-damping-moment derivatives for these models, these derivatives are more accurately determined than their side-force counterparts. Also, from the uncertainties cited in the previous section, derivative estimates for the larger model are more precise than those for the smaller model. This occurs because the models had nearly identical magnetic forces and moments while the aerodynamic forces were larger for the larger model.

A principal factor limiting measurement accuracy in these experiments was an experimental upper limit on wind-tunnel dynamic pressure, above which the model could not be maintained in stable support. This limit was imposed by the limited lateral force capability of the suspension apparatus. That is, due to slight angularities in the wind tunnel flow and in the model's magnetization vector (due to small, but always present residual magnetism in the core) and, in particular, due to time-variation of this angularity caused by flow turbulence and slow rolling of the model, above a certain dynamic pressure the suspension system's

---

*The axial stations of the moment-reference point for the $C_{m_{\dot{\alpha}}} + C_{m_q}$ data from Ref.13 differ slightly from that for the present data. The $C_{z_{\dot{\alpha}}} + C_{z_q}$ data necessary to to convert these data are not available. Despite this lack, the $C_{m_{\dot{\alpha}}} + C_{m_q}$ value for the 155 mm Shell M101 compares reasonably well with the present result. The $C_{m_{\dot{\alpha}}} + C_{m_q}$ value for the 1/12-th scale model, as suggested by the authors, is apparently in error.

Table 1 Data Comparisons, 5-Caliber Model

Model	A	B	C	D	E	F	F	G	H	I	Present
Ref.	(8)	(9)	(9)	(10)	(11)	(12)	(12)	(13)	(13)	(7)	Tests
$Re_d \times 10^5$	4.4	5.0	5.0	6.4	5.3	2.2	2.4	2.1	1.8	0.13	0.13
M	0.15	0.2	0.2	0.26	0.5	0.2	0.4	0.6	0.7	0.07	0.07
C_{z_α}	-1.98	-2.08	-2.42	-2.21	-1.8	-2.04	-2.04	-1.8	-1.8	-1.84	-1.5 ±0.9
C_{m_α} †	4.19	1.75	2.05	3.7	4.31	4.91	4.51	4.09	4.01	3.28	3.6 ±0.1
C_x	---	---	---	---	---	---	---	-0.14	-0.13	-0.25 § -0.21 ¶	-0.21 ±0.005
$C_{m_{\dot\alpha}}+C_{m_q}$ †	---	---	---	---	---	---	---	-10.0 τ	4.6 ω	-3.63	-3.3 ±1.5
$C_{z_{\dot\alpha}}+C_{z_q}$	---	---	---	---	---	---	---	---	---	-8.27	-2.2 ±2.0

A= 5 caliber Army-Navy Spinner Rocket with secant ogive nose.
B= 4.4 cal. with tangent ogive nose.
C= 5.9 cal. with tangent ogive nose.
D= 5 cal. with secant ogive nose.
E= 5.6 cal. with truncated conical nose, boat tail, and spiral grooves.
F= 3.8 cal. 20 mm Projectile with blunt conical nose, circumferential grooves, and projections.
G= 4.5 cal. 155 mm Shell M101 with tangent ogive nose, boat tail, and spiral grooves.
H= 1/12 scaled model of G.
I= Analytical estimate for 5 cal. model with conical nose.

†About a point 3.4 calibers behind nose.
§Assuming fully turbulent flow.
¶Assuming fully laminar flow.
τAbout a point 3 calibers behind nose.
ωAbout a point 2.8 calibers behind nose.

Table 2 Data Comparisons, 7-Caliber Model

Model	A	B	C	D	E	F	Present
Ref.	(8)	(8)	(8)	(9)	(10)	(7)	Tests
$Re_d \times 10^5$	4.3	7.3	7.3	5.0	6.4	0.13	0.13
M	0.15	0.25	0.25	0.2	0.26	0.07	0.07
C_{z_α}	-1.81	-2.53	-2.48	-2.76	-2.18	-1.98	-2.6±0.3
C_{m_α} †	6.58	6.17	7.42	6.97	5.87	6.97	5.9±0.15
C_x	---	---	---	---	---	-0.269 § -0.209 ¶	-0.223 ±0.005
$C_{m_{\dot\alpha}}+C_{m_q}$ †	---	---	---	---	---	-11.6	-14.6±3.0
$C_{z_{\dot\alpha}}+C_{z_q}$	---	---	---	---	---	-13.7	-4.1±4.0

A= 7 caliber Army-Navy Spinner Rocket with secant ogive nose.
B= 7 cal. with conical nose.
C= 7 cal. with tangent ogive nose.
D= 7.1 cal. with tangent ogive nose.
E= 7 cal. with secant ogive nose.
F= Analytical estimate for 7-cal. model with conical nose.

†About a point 4.6 calibers behind nose.
§Assuming fully turbulent flow.
¶Assuming fully laminar flow.

lateral force capability was insufficient to both excite the model's motion and maintain it in stable support. The higher the dynamic pressure, however, the larger the differences between the model's flow-off and flow-on response and thus the stability derivatives can be measured more precisely. Even with this limitation, however, the present data are of comparable accuracy to those obtained by conventional means with considerably larger models and at generally higher flow dynamic pressures. Moreover, the present data are surely free of the fluid-mechanics aspects of sting interference and, with the excellent fits between the measured amplitudes and the modeling expression, systematic errors in the aerodynamic derivative estimates due to errors in the model are surely no larger than those corresponding to the scatter in the response data.

With minor alteration of the apparatus and the technique, these experiments could be extended to somewhat higher flow speeds, larger models, to finned models, and probably to rapidly spinning models. By using dummy stings, this technique could also be used to study sting interference.

REFERENCES

1. Copeland, A.B., Covert, E.E., and Peterson, R.A., "Wind-Tunnel Measurement at M = 4.28 of Some Static and Dynamic Aerodynamic Characteristics of Finned Missiles Suspended Magnetically," J. Spacecraft, Vol. 5, No. 7, July 1968, pp. 838-842.

2. Vlajinac, M. and Gilliam, G.D., "Aerodynamic Testing of Conical Configurations Using a Magnetic Suspension System," MIT, Aerospace Research Laboratories Report ARL 70-0067, 1970.

3. Goodyer, M.J., "Some Force and Moment Measurements Using Magnetically Suspended Models in a Low Speed Wind Tunnel," in Summary of ARL Symposium on Magnetic Wind Tunnel Model Suspension and Balance Systems, Dayton University, Dayton, Ohio, July 1966 (F.L.Daum, Editor).

4. Judd,M.,"The Magnetic Suspension System as a Wind Tunnel Dynamic Balance," IEEE, International Congress on Instrumentation in Aerospace Simulation Facilities Record, 1969, pp.198-206.

5. Bharathan, D. "Aerodynamic Stability Testing with Magnetically Suspended Models," Ph.D. Dissertation, University of Virginia, Charlottesville, Virginia, 1976.

6. Moore, R.H. and Ziegler, R.K.,"The Solution of the General Least-Square Problem with Special Reference to High-Speed Computers," Los Alamos Scientific Laboratory Report LA 2367, Los Alamos, New Mexico, October 1959.

7. Finck, R.D. and Hoak, D.E.," USAF Stability and Control DATCOM ," Flight Control Division, Air Force Flight Dynamics Laboratory, Wright-Patterson Air Force Base, Dayton Ohio, October 1954.

8. Greene, J.E.,"Static Stability and Magnus Characteristics of the 5-caliber and 7-caliber Army-Navy Spinner Rocket at Low Subsonic Speeds," NAVORD Report 3884, December 1954.

9. Fletcher, C.A.J., " Investigation of the Magnus Characteristics of a Spinning Inclined Ogive-Cylinder Body at M=0.2," Australian Defense Scientific Service TN PSA 159, October 1969 (N70-35050).

10. Nielson, G.I.T. and Platou, A.S., " The Effects of Conical Boat-Tails on the Magnus Characteristics of Projectiles at Subsonic and Transonic Speeds," Ballistic Research Laboratories Report 1720, July 1974.

11. Platou, A.S. and Nielson, G.I.T., " Some Aerodynamic Charateristics of the Artillary Projectile XM 549 ," Ballistic Research Laboratories Memorandum Report No. 2284, April 1974.

12. Sieron, T.R., " The Magnus Characteristics of the 20 mm and 30 mm Projectiles in the Transonic Speed Range," Wright Air Development Center TN 59-320, October 1959.

13. Karpov, B.G. and Schmidt, L.E., " The Aerodynamic Properties of the 155 mm Shell M-101 from Free-Flight-Range Tests of Full Scale and 1/12 Scale Models," Ballistic Research Laboratories Memorandum Report 1582, June 1964.

UNCLASSIFIED
SECURITY CLASSIFICATION OF THIS PAGE (When Data Entered)

REPORT DOCUMENTATION PAGE

READ INSTRUCTIONS BEFORE COMPLETING FORM

1. REPORT NUMBER: AFOSR - TR - 77 - 0666	2. GOVT ACCESSION NO.
3. RECIPIENT'S CATALOG NUMBER	
4. TITLE (and Subtitle): STABILITY DERIVATIVE MEASUREMENTS FOR MAGNETICALLY SUSPENDED CONE-CYLINDER MODELS,	5. TYPE OF REPORT & PERIOD COVERED: INTERIM
	6. PERFORMING ORG. REPORT NUMBER
7. AUTHOR(s): D/BHARATHAN, S S FISHER	8. CONTRACT OR GRANT NUMBER(s): AF-AFOSR-2705-74, ~~AFOSR 74-2705~~
9. PERFORMING ORGANIZATION NAME AND ADDRESS: UNIVERSITY OF VIRGINIA, ENGINEERING AND APPLIED SCIENCE, CHARLOTTESVILLE, VA 22901	10. PROGRAM ELEMENT, PROJECT, TASK AREA & WORK UNIT NUMBERS: 9783-06, 61102F
11. CONTROLLING OFFICE NAME AND ADDRESS: AIR FORCE OFFICE OF SCIENTIFIC RESEARCH/NA, BLDG 410, BOLLING AIR FORCE BASE, D C 20332	12. REPORT DATE: Jan 77
	13. NUMBER OF PAGES: 9 (12 pp.)
14. MONITORING AGENCY NAME & ADDRESS (if different from Controlling Office)	15. SECURITY CLASS. (of this report): UNCLASSIFIED
	15a. DECLASSIFICATION/DOWNGRADING SCHEDULE

16. DISTRIBUTION STATEMENT (of this Report)

Approved for public release; distribution unlimited.

17. DISTRIBUTION STATEMENT (of the abstract entered in Block 20, if different from Report)

18. SUPPLEMENTARY NOTES

AIAA Aerospace Sciences Meeting 15th Los Angeles, CA pp1-8 24-26 Jan 77

19. KEY WORDS (Continue on reverse side if necessary and identify by block number)

DYNAMIC STABILITY
MAGNETIC SUSPENSION
MAGNETIC FORCE BALANCE

20. ABSTRACT (Continue on reverse side if necessary and identify by block number)

In an initial feasibility study, the stability derivatives, C_{m_α}, $C_{m_{\dot\alpha}} + C_{m_q}$ C_{z_α} and $C_{z_{\dot\alpha}} + C_{z_q}$ for 5- and 7-caliber cone-cylinder models have been measured at M= 0.071 and Re = 1.3×10^4 by suspending each model electromagnetically in a small subsonic wind tunnel , forcing it in periodic, combined pitching/heaving motion at frequencies near pitch resonance, and comparing its frequency response with flow to that without flow. Drag coefficients are measured as well. The apparatus and techniques employed are described, the analytical model used to

DD FORM 1 JAN 73 1473 EDITION OF 1 NOV 65 IS OBSOLETE

UNCLASSIFIED 401 975
SECURITY CLASSIFICATION OF THIS PAGE (When Data Entered)

extract the derivatives from the response data is outlined, typical response data are shown, comparisons are made with conventionally obtained, similar data from other facilities, and a general assessment of the technique is made.